Battery Charger for Electric Vehicles with High-Efficiency Bridgeless Single-Power Conversion

RONDI BABU[1]V.YOGITHA[2]G.VAMSHI KRISHNA[3]A.NAVEEN REDDY[4] CH.JYOSHNA[5]

[1]Associate Professor, Department of EEE, Jyothishmathi institute of technology and science, Nustulapur, Karimnagar, TS, India

[2,3,4,5]UG students, Department of EEE, Jyothishmathi institute of technology and science,Nustulapur, Karimnagar, TS, India

Abstract: A high power factor and high efficiency are necessary for charging the batteries of light electric vehicles. A bridgeless single-power conversion battery charger with an isolated step-up AC-DC converter and a series resonance circuit is presented in this work to suit this need. Using a series-resonance circuit instead of a bridge decreases the output diodes' reverse recovery losses and the conduction losses associated with the input diode rectifier. In addition, the transformer's bidirectional core excitation is made possible by direct and series-resonance current injection, allowing for higher power output. Feedback linearization is used to design a control method that allows the suggested charger to manage output power while also correcting for power factor. The great efficiency and high-power factor of this circuit can be attributed to its simple design.

Keywords: Power factor correction, Electric vehicle, AC-DC converter

I.INTRODUCTION

Environmental pollution can be significantly reduced by various environmentally friendly vehicles such as electric cars (EVs), plug-in hybrid electric cars (PHEVs), and other plug-in hybrid electric vehicles (PHEVs) that have gained popularity in recent years [1–3]. For an EV, the propulsion batteries are recharged using an on-board charger, which is a critical component of an EV's design. [4] The charger's power-conversion efficiency and power quality are used to measure its performance (i.e., total harmonic distortion and power factor). In addition, the charger must be tiny, light, and long-lasting because it is built into the electric vehicle. Isolated AC-DC converters with two-stage structures based on the PFC stage and DC-DC power conversion stages are used in conventional onboard chargers for electric vehicles [5]– [7].

DC-DC power conversion stage, which is usually an isolated high-frequency isolated DC-DC converter, regulates the output power and offers galvanic isolation for user safety. This design provides advantages such as being able to accept a wide range of input voltages, giving a high-power factor, and maintaining a stable output power. There are various downsides to a two-stage power processing system, including low efficiency and circuit complexity due to its two power-processing stages. Additionally, the intermediate DC-link capacitor that filters power fluctuations is a severe negative. There is also significant power loss and reduced capacitor lifetime due to a high current flowing through the intermediate dc-link capacitor (failure) (10) and (11). Single-stage techniques are being developed to replace two-stage architectures in order to eliminate the PFC stage and lower the dc-link capacitance [12], [13]. The PFC stage and the DC-DC stage are combined in single-stage converters with a DC-link capacitor by sharing the switches.

Despite this, the DC-link voltage can be more than twice the grid voltage, which necessitates the use of high-voltage switches that result in substantial switching and conduction losses. As a result, the power factor might be influenced by changes in the grid voltage or load conditions because PFC is performed without an additional PFC controller.

Single-stage resonance converters with inherent PFC and current-fed full-bridge converters have been introduced to attain a high-power factor without a PFC stage and a DC-link capacitor [15].

Because a DC link capacitor isn't needed with these converters, any issues it can cause are gone. Using the appropriate PFC-control methods, a power factor close to unity can be attained. Many components and an input bridge diode necessitate additional heat management in single-stage converters, resulting in substantial conduction losses. The use of a two-stage boost-fly back converter and a half-bridge PFC converter in a single-stage bridgeless topology has been studied to address these issues. Such converters, on the other hand, are only suited for low-power applications because to the large electrical stresses imposed by the applicable topologies. Because of this, isolated bridgeless type converters with large power capabilities (>1 kW) have received little research attention. This work presents high-efficiency bridgeless single-power-conversion battery chargers in order to overcome this issue.

PFC control and power output regulation are achieved using a bridgeless step-up ACDC converter that is isolated from the rest of the circuit. The bridge diode's heat management and conduction losses are reduced by using a bridgeless design. With its zero-current switching (ZCS) and high-power capacity provided by the secondary side's series-resonance circuit, the output diodes' reverse-recovery difficulty is reduced. An additional benefit is that, since input and output energy are dispersed without a buffer, efficiency is increased.

A feedback linearization-based control technique is used to produce a high-power factor without the need for an additional PFC circuit. The proposed charger is able to rectify the power factor and regulate output power through a single power conversion thanks to this control algorithm. Consequently, it is a good choice for EVs that require high charging efficiency and high-quality power as an on-board charger.

II PROPOSED SYSTEM

Explanation of proposed charger

Fig. 1 depicts the proposed single-power-conversion battery charger's circuit architecture. The primary side of the transformer T has two diodes and two switches. To maintain a grid voltage vg, the diodes Dp (Dn) and Dn(P) alternately conduct throughout each half-cycle of grid period Tg. In the positive half-cycle, switch S2(S1) is constantly on, and switch S1(S2) is driven at a high frequency during this time. One switch operates at a higher frequency, whereas the other one is always on. As a result, just one switch suffers switching losses.

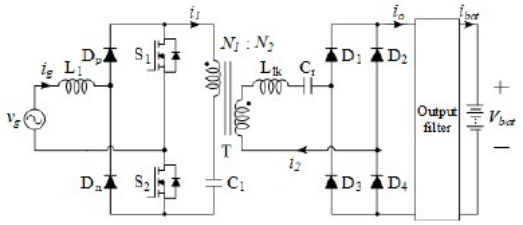

Fig. 1. Proposed single power conversion without a bridge DC-to-AC power supply

Output diodes and a series-resonance circuit with a leakage inductance Llk and a resonant capacitor Cr make up the secondary side of the circuit. The ZCS provided by the series resonance reduces the problem of reverse recovery of the output diodes. It doesn't matter if switches S1 and S2 are on or off while using the suggested charger because it influences the bidirectional core excitation It is possible to transfer energy from one side of a circuit to another by using a series-resonance circuit. The primary side inductors L1 and Lm feed energy into the secondary side while the high-frequency switch is off. The proposed converter is able to handle a lot of power because of this feature. Galvanic isolation is ensured by using a high-frequency transformer, which is also utilised to protect users.

Principles of Operation

Using the following assumptions, this section investigates the charger's steady-state performance: Exception: body diodes, which make the switches S1 and S2 less than optimal. 2) Because Ts is substantially shorter than grid period Tg, the grid voltage vg is regarded constant throughout each switching period Ts. Because the battery's capacitance is sufficiently big, the voltage Vbat remains constant. It is described as an ideal transformer with a magnetic inductance Lm and a leakage inductance Llk. The switching time Ts is separated into three operating modes based on the state of the switches and the output diodes for steady-state operation in the positive and negative half cycles. As a result, the charger under consideration operates symmetrically in both the positive and negative half-cycles. As a result, only the positive half of the cycle is taken into account in our investigation. On the left, you can see the

analogous circuits and, on the right, you can see the theoretical waveform for each operating mode.

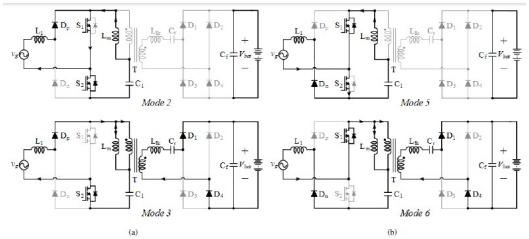

Fig. 2. The suggested charger's several modes of operation (a) Half-cycle of grid voltage in the positive direction. (b) Grid voltage in the negative half-cycle.

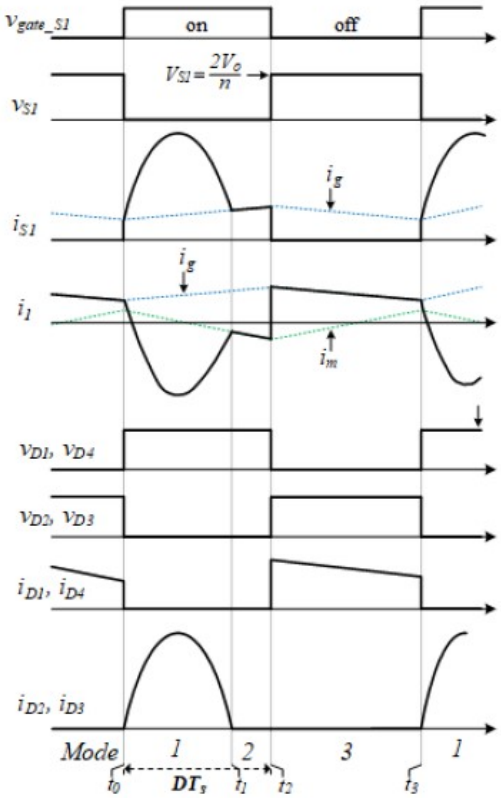

Fig. 3. Schematic diagram of the charger's theoretical waveforms

III.CONTROL STRATEGY

The suggested charger corrects the power factor without a PFC stage or auxiliary circuit by changing the duty ratio D of the switches. However, high-quality power delivery is complicated by the nonlinearity of the duty ratio D and grid current gi. A feedback linearization technique for the proposed charger is introduced in this part and provides adequate control of the proposed charger.

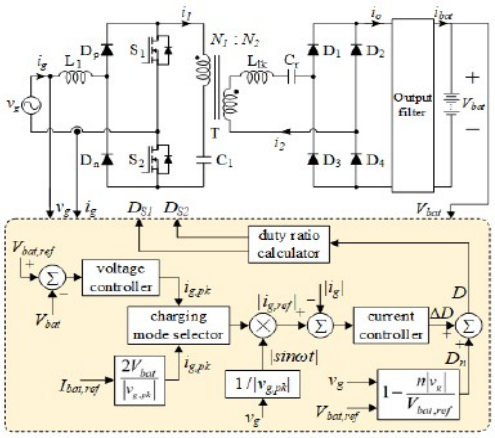

Fig. 4. The suggested charger's control block diagram.

Fig. 4 depicts a block diagram of the control method suggested in this paper. For L1's average voltage equation, the duty ratio D of switches and the variance in the grid current ig are used.

$$L_1 \frac{\Delta I_i}{T_S} = V_i D - \left(\frac{V_{Cr} + V_{bat}}{n} \right)(1 - D) \quad (1)$$

The duty ratio can be calculated by combining as follows:

$$D = \left(1 - \frac{n \mid v_g \mid}{2V_{bat,ref}} \right) + \frac{nL_i}{2V_{bat,ref} T_S} \Delta i_g \quad (2)$$

where Vbat; ref is the battery's reference voltage. The nominal duty ratio Dn and duty ratio variation D can be calculated using Eq. (3).

$$D_n = \left(1 - \frac{n \mid v_g \mid}{2V_{bat,ref}} \right), \Delta D = \frac{nL_i}{2V_{bat,ref} T_S} \Delta i_g \quad (3)$$

Dn can be detached from Eq. (2) and used as a feed forward controller from Eq. (3). Improves dynamic responsiveness in controlled system by relieving load on voltage and current regulator through feed-forward control. In addition, the relationship between D and the current variation iL1, which now equals the grid current variation ig, is linearized when the nominal duty ratio Dn is decoupled from the duty-ratio variation D. The nonlinear system is now a first-order linear system because ig is linear in D.

TABLE I
The SIMULATION PERFORMANCE AND PARTS.

Parameters	Symbols	Value
Grid voltage	v_g	120-240 V_{rms}
Grid frequency	f_g	60 Hz
Nominal battery voltage	V_{bat}	360 V
Rated output power	P_o	1.7 kW
Switching frequency	f_s	70 kHz
Primary inductance	L_1	1.5 mH
Primary capacitance	C_1	6.6 μF
Magnetizing inductance	L_m	450 μH
Secondary leakage inductance	L_{lk}	1.6μH
Transformer turns ratio	$N_1 : N_2$	24:36
Resonant capacitance	C_r	1 μF
Output filter capacitance	C_f	3.3 μF
Output filter inductance	L_f	40 μH

Fig. 4 depicts the suggested charger's control block diagram. Voltage regulators of the proportional-integral type seek to compensate for any difference in battery voltage Vbat and the target battery voltage Vbat;ref by calculating the difference. The voltage controller provides the amplitude of the grid current reference i*g -pk. ig ;pk, on the other hand, is computed using the following relationship between the input and output power in the constant current charging mode:

$$i^*_{g,pk} = \frac{2V_{bat} i_{bat,ref}}{\mid v_{g,pk} \mid} \quad (4)$$

where ibat;ref is the required battery voltage. Multiplying the grid current reference's amplitude by vg=vg;pk, which is the grid voltage's peak value, yields the reference grid current i*g ;ref. A high-power factor is achieved by matching the phase of the reference grid current i*g; ref to the phase of the grid voltage vg. By varying the duty ratio, the proportional current controller tries to compensate for the difference between the measured current and the reference current.

As a result, the nominal duty ratio Dn and the duty ratio variation D are added to arrive at the duty ratio D. S1 is turned on when D is applied to switch S1, and S2 is always on when D is applied to switch S1. Similarly, D is applied to S2 in the negative half cycle.

IV.SIMULATION RESULTS

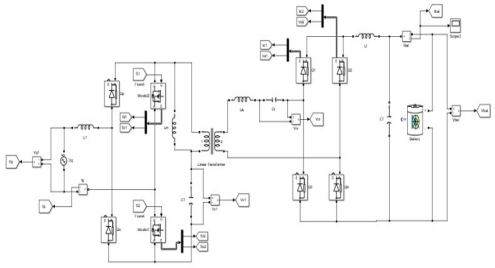

Fig.5 MATLAB/SIMULINK circuit of the proposed bridgeless single power conversion AC/DC converter

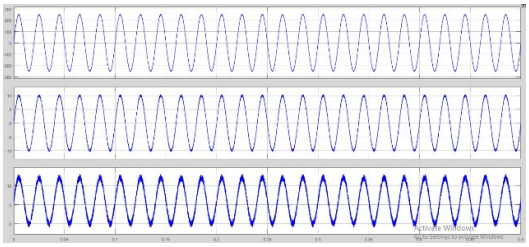

Fig. 6. Simulation results of voltage vg, current ig of grid and battery current ibat

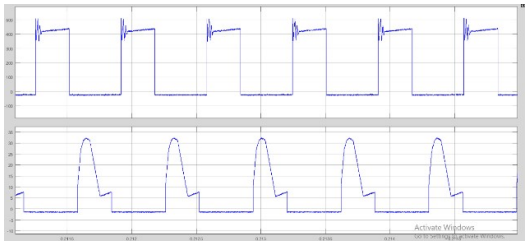

(a)

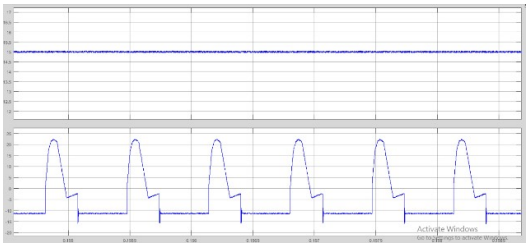

(b)

Fig. 7. simulation results for the voltage stress and current of the switches for positive half cycle (a) S1. (b) S2.,

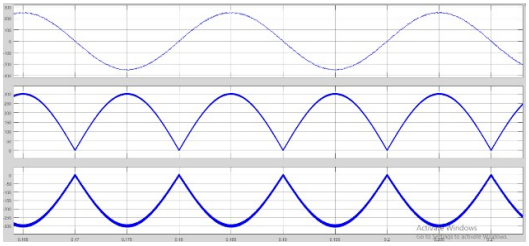

Fig. 8. Simulation results for
the grid voltage vg, the main capacitor voltage vC1,
and the resonant capacitor voltage vCr

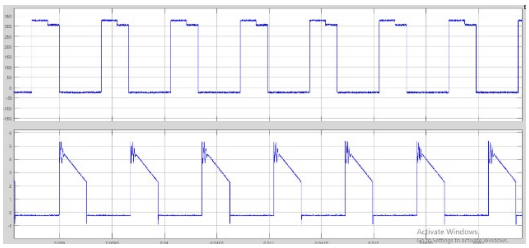

(a)

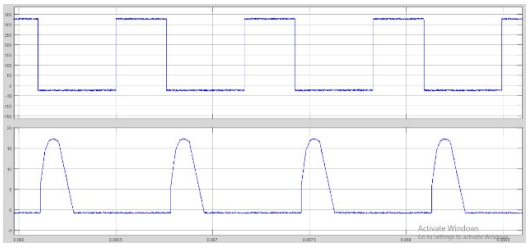

(b)

Fig. 9. Simulation results for the voltage stress and current of output diodes a) D1. b) D2.

CONCLUSION

Bridgeless battery chargers for light EVs are proposed in this work, which analyses their theoretical and experimental performance. The usage of a series resonance circuit enables ZCS and alleviates the reverse recovery problem for output diodes by eliminating the input bridge diode. Transformers with bidirectional core excitation have a larger power capacity than those with bridgeless converters in the past. Because the proposed charger uses an electrolytic capacitorless method with a sinusoidal-like dc current on the battery side, the incoming ac power is immediately transmitted to the battery side, improving efficiency. As an added benefit, the suggested control method allows the charger to adjust output while also correcting the power factor. The proposed charger has high efficiency and high-power quality as a result of these features. The simple circuit topology and soft-switching features for the output diodes result in a maximum efficiency of 96.2 percent. Additionally, a power factor close to unity is achieved for a global grid voltage when the control algorithm is utilized. Because EVs require great charging efficiency, a high-power factor, and a simple structure, the suggested charger with its control algorithm is an ideal answer.

REFERENCES

[1] S. Haghbin, S. Lundmark, M. Alakula, and O. Carlson, “Grid-connected integrated battery chargers in vehicle applications: Review and new solution,” IEEE Transactions on Industrial Electronics, vol. 60, no. 2, pp. 459–473, 2013.

[2] M. Yilmaz and P. T. Krein, “Review of battery charger topologies, charging power levels, and infrastructure for plug-in electric and hybrid vehicles,” IEEE Transactions on Power Electronics, vol. 28, no. 5, pp. 2151–2169, 2013.

[3] A. Khaligh and S. Dusmez, “Comprehensive topological analysis of conductive and inductive charging solutions for plug-in electric vehicles,” IEEE Transactions on Vehicular Technology, vol. 61, no. 8, pp. 3475– 3489, 2012.

[4] S.-G. Jeong, W.-J. Cha, S.-H. Lee, J.-M. Kwon, and B.-H. Kwon, “Electrolytic Capacitor-Less Single-Power-Conversion On-Board Charger With High Efficiency,” IEEE Transactions on Industrial Electronics, vol. 63, no. 12, pp. 7488–7497, 2016.

[5] B. Whitaker, A. Barkley, Z. Cole, B. Passmore, D. Martin, T. R. McNutt, A. B. Lostetter, J. S. Lee, and K. Shiozaki, “A high-density, highefficiency, isolated on-board vehicle battery charger utilizing silicon carbide power devices,” IEEE Transactions on Power Electronics, vol. 29, no. 5, pp. 2606–2617, 2014.

[6] D. S. Gautam, F. Musavi, M. Edington, W. Eberle, and W. G. Dunford, “An automotive onboard 3.3-kW battery charger for PHEV application,” IEEE Transactions on Vehicular Technology, vol. 61, no. 8, pp. 3466– 3474, 2012.

[7] S. Kim and F.-S. Kang, “Multifunctional onboard battery charger for plug-in electric vehicles,” IEEE Transactions on Industrial Electronics, vol. 62, no. 6, pp. 3460–3472, 2015.

[8] K. Yao, Y. Wang, J. Guo, and K. Chen, “Critical Conduction Mode Boost PFC Converter with Fixed Switching Frequency Control,” IEEE Transactions on Power Electronics, 2017.

[9] T. Mishima, K. Akamatsu, and M. Nakaoka, “A high frequency-link secondary-side phase-shifted full-range soft-switching PWM DC-DC converter with ZCS active rectifier for EV battery chargers,” IEEE Transactions on Power Electronics, vol. 28, no. 12, pp. 5758–5773, 2013.

[10] M. Kwon and S. Choi, “An Electrolytic Capacitorless Bidirectional EV Charger for V2G and V2H Applications,” IEEE Transactions on Power Electronics, vol. 32, no. 9, pp. 6792–6799, 2017.

[11] K.-M. Yoo, K.-D. Kim, and J.-Y. Lee, “Single-and three-phase PHEV onboard battery charger using small link capacitor,” IEEE Transactions on Industrial Electronics, vol. 60, no. 8, pp. 3136–3144, 2013.

[12] L. Wang, B. Zhang, and D. Qiu, “A Novel Valley-Fill Single-Stage Boost-Forward Converter With Optimized Performance in Universal- Line Range for Dimmable LED Lighting,” IEEE Transactions on Industrial Electronics, vol. 64, no. 4, pp. 2770–2778, 2017.

[13] Y. Wang, N. Qi, Y. Guan, C. Cecati, and D. Xu, “A single-stage LED driver based on SEPIC and LLC circuits,” IEEE Transactions on Industrial Electronics, vol. 64, no. 7, pp. 5766–5776, 2017.

[14] G. Moschopoulos and P. Jain, “Single-phase single-stage power-factorcorrected converter topologies,” IEEE Transactions on Industrial Electronics, vol. 52, no. 1, pp. 23–35, 2005.

[15] S. Li, J. Deng, and C. C. Mi, “Single-stage resonant battery charger with inherent power factor correction for electric vehicles,” IEEE Transactions on Vehicular Technology, vol. 62, no. 9, pp. 4336–4344, 2013.